GEOLOGY

Barium isotope evidence for pervasive sediment recycling in the upper mantle

Sune G. Nielsen[1,2]*, Tristan J. Horner[1,3], Helena V. Pryer[1,3], Jerzy Blusztajn[1,2], Yunchao Shu[1,2,4,5], Mark D. Kurz[3], Véronique Le Roux[2]

The upper mantle, as sampled by mid-ocean ridge basalts (MORBs), exhibits significant chemical variability unrelated to mechanisms of melt extraction at ridges. We show that barium isotope variations in global MORBs vary systematically with radiogenic isotopes and trace element ratios, which reflects mixing between depleted and enriched MORB melts. In addition, modern sediments and enriched MORBs share similar Ba isotope signatures. Using modeling, we show that addition of ~0.1% by weight of sediment components into the depleted mantle in subduction zones must impart a sedimentary Ba signature to the overlying mantle and induce low-degree melting that produces the enriched MORB reservoir. Subsequently, these enriched domains convect toward mid-ocean ridges and produce radiogenic isotope variation typical of enriched MORBs. This mechanism can explain the chemical and isotopic features of enriched MORBs and provide strong evidence for pervasive sediment recycling in the upper mantle.

INTRODUCTION

The chemistry of oceanic island basalts (OIBs) is generally thought to reflect the influence of recycled material that was introduced into the mantle during subduction of crustal lithologies and brought back to the surface via plumes (*1*, *2*). Although the chemistry of mid-ocean ridge basalt (MORB) is relatively homogeneous compared to that of OIBs, the source region of MORB (the depleted MORB mantle or DMM) also displays substantial chemical and isotopic variation (*2*). For example, enriched MORB (E-MORB) has high concentrations of incompatible elements, fractionated trace element ratios (for example, high La/Sm and Ba/La), and more radiogenic $^{87}Sr/^{86}Sr$ isotope ratios compared to depleted MORB (D-MORB) (*3*). Conversely, major element differences between MORB types are subtle and likely relate to higher water and alkali content in E-MORB, rather than mechanisms of melt extraction at the ridge (*4*–*7*). Although evidence from He isotopes has suggested that some of this variation is likely related to the introduction of primordial lower mantle material into the upper mantle (*8*–*11*), differences between E-MORB and D-MORB cannot be explained by the influence of deep mantle reservoirs (*3*, *12*). Therefore, a substantial portion of the DMM heterogeneity is probably related either to (i) internal redistribution of different components, for example, through delamination of lithospheric mantle (*13*), fluid metasomatism, and melt-rock reactions (*14*, *15*) or to (ii) direct exchange between DMM and surface reservoirs such as addition of sediments and altered oceanic crust (AOC) to the upper mantle in subduction zones (*5*, *16*). From a global perspective, it is difficult to distinguish between these different hypotheses because most of these models can theoretically account for the trace element and radiogenic isotope differences observed in the spectrum between E-MORB and D-MORB. Many types of geochemical measurements, such as trace element and radiogenic isotope ratios, have struggled to discriminate between these models. A potential means to this end is by using novel stable isotope tools because processes that cause significant stable isotope fractionation are primarily found in low-temperature environments (for example, sediment precipitation and hydrothermal alteration). Therefore, stable isotopes are potentially more direct tracers of recycling processes than trace elements and radiogenic isotopes.

Here, we use Ba (barium) stable isotope measurements to investigate the origin of DMM heterogeneity. Barium is a highly incompatible element that is enriched up to 100 times more in E-MORB compared to normal MORB (N-MORB) (*3*, *17*). Barium is also fluid mobile (*18*) and is one of the most commonly used elements to track slab-derived fluids in subduction zones (*19*). In addition, Ba can be highly enriched in sediments (*20*), up to 10,000 times compared to DMM (Fig. 1). Thus, the strong Ba enrichments found in E-MORB could be explained by low-degree melting occurring within the mantle, by fluid fluxing in subduction zones, and/or via introduction into the mantle of Ba-rich crustal components such as sediments. Here, we use Ba isotopes to investigate the origin of DMM heterogeneity. The new data provide the first strong evidence for pervasive global sediment recycling in the MORB source away from plume influence, and we show that the subducted sediment-rich material plays a key role in the formation of the E-MORB reservoir in subduction zones.

Barium isotope fractionation and cycling in surface environments

Barium has seven stable isotopes (130, 132, 134, 135, 136, 137, and 138). Studies of high-precision stable Ba isotopes were only recently developed (*21*) with almost all subsequent studies focusing on the Ba isotope systematics of low-temperature processes and environments such as seawater (*22*–*24*), experimental barite precipitation (*21*), isotope fractionation during plant "biolifting" (*25*), and during diffusive transport (*26*). Barium isotope compositions have been reported using the conventional δ notation, albeit referenced to different standards and using different sets of isotopes, most commonly as $^{138}Ba/^{134}Ba$ or $^{137}Ba/^{134}Ba$. In principle, all these notations reflect the same intrinsic isotope variation and can easily be recalculated to the same notation. However, as in our previous studies, we report here our values with the $^{138}Ba/^{134}Ba$ ratio relative to the National Institute of Standards and Technology (NIST) 3104a standard:

$$\delta^{138/134}Ba_{NIST} = 1000 \times \left(\left({}^{138}Ba/{}^{134}Ba_{sample}/{}^{138}Ba/{}^{134}Ba_{NIST}\right) - 1\right)$$

[1]NIRVANA (Non-traditional Isotope Research for Advanced Novel Applications) Laboratories, Woods Hole Oceanographic Institution, Woods Hole, MA 02543, USA. [2]Department of Geology and Geophysics, Woods Hole Oceanographic Institution, Woods Hole, MA 02543, USA. [3]Department of Marine Chemistry and Geochemistry, Woods Hole Oceanographic Institution, Woods Hole, MA 02543, USA. [4]Institute of Oceanology, Chinese Academy of Sciences, Qingdao, China. [5]University of Chinese Academy of Sciences, Beijing, China.
*Corresponding author. Email: snielsen@whoi.edu

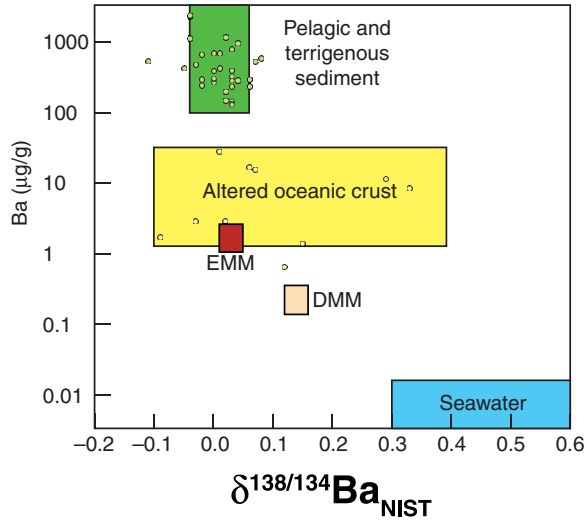

Fig. 1. Summary of Ba concentrations and isotope compositions for different reservoirs relevant for crustal recycling. Sources for the data are cited in the text or listed in table S4. Note the logarithmic scale on the *y* axis. EMM, enriched MORB mantle; NIST, National Institute of Standards and Technology.

One of the primary findings of recent Ba isotope studies in low-temperature environments is that precipitation of barite appears to be the primary mediator of Ba isotope fractionation in the open ocean (*22*). Specifically, precipitation of barite is associated with a fractionation factor of $\alpha \sim 0.9995$ [that is, barites are enriched in the light isotopes relative to seawater by ≈0.5 per mil (‰)], which has been shown theoretically (*27*) and experimentally (*21*) and inferred for marine barites precipitated from seawater (*22*, *28*). The effects of this isotope fractionation causes a distinct structure of Ba isotopes in the ocean whereby the surface ocean in oligotrophic regions (such as the geographically extensive gyres of the South Atlantic or North Pacific) is depleted in Ba (~5.5 ng/g) (*29*) and characterized by heavy Ba isotope compositions of $\delta^{138/134}Ba_{NIST} \approx +0.6$, whereas deep waters rich in nutrients have higher Ba concentrations (>14 ng/g) (*29*) and $\delta^{138/134}Ba_{NIST} \approx +0.3$. Most deep-sea marine sediments are significantly enriched in Ba from deposition of barite from the water column (*20*), which, given the constant Ba isotope fractionation between barite and seawater and the geographically extensive oligotrophic regions in the ocean, results in most bulk sediments exhibiting a relatively narrow range of Ba isotope compositions close to $\delta^{138/134}Ba_{NIST} \sim 0$ [see (*28*) and Fig. 1].

The Ba isotope composition of seawater likely also significantly influences AOC through hydrothermal circulation of seawater at low temperatures. During low-temperature hydrothermal alteration, Ba is not significantly deposited into secondary minerals or extracted from the oceanic crust (*30*, *31*). Similar to Ba, strontium (Sr) also shows only minor deviation in concentrations from unaltered to AOC (*30*, *31*), but studies have shown substantial isotopic exchange between seawater and Sr in oceanic crust such that AOC partially inherits the Sr isotope composition of seawater (*30*, *32*). Given the geochemical similarity of Ba and Sr in terms of charge and ionic radius (*33*), it is likely that a similar Ba isotopic exchange also takes place between seawater and the oceanic crust, in which case AOC will partially inherit the Ba isotope composition of the seawater circulating through it. Since the range of seawater Ba isotope composition is $\delta^{138/134}Ba_{NIST} \approx +0.3$ to +0.6‰, it is expected that these compositions form one boundary composition for AOC, with the other represented by unaltered MORBs, which is consistent with recent reports of Ba isotopes in AOC (*34*). Collectively, these observations suggest that distinct Ba isotope compositions are imprinted into surface reservoirs such as sediments and AOC, which can be exploited when studying processes of material exchange between surface and mantle reservoirs (Fig. 1).

RESULTS

We report Ba, Sr, and Nd isotope compositions and trace elements for 21 MORB samples (tables S1 and S2). The MORB samples studied were selected on the basis of three criteria: (i) Helium isotope compositions are almost uniform at the normal mantle value and exhibit $^3He/^4He = 7.9\ R_A$ (±0.5 SD; table S1) within error of the average normal mantle (*9*–*11*, *35*, *36*). (ii) Magnesium concentrations for most samples are higher than 7.5% (table S3), which suggests that fractional crystallization of these melts was relatively minor. (iii) The samples cover the main spreading centers of the global mid-ocean ridge system, which is intended to reveal whether there are any systematic large geographic differences in Ba isotope composition of MORB.

The samples cover most main spreading centers on the globe (Fig. 2 and table S1) and almost the entire range of MORB compositions (*37*), from highly depleted to enriched, which is illustrated by the large variation observed in $^{87}Sr/^{86}Sr$, $^{143}Nd/^{144}Nd$, and La/Sm (Fig. 3). Most of the samples originate from the Mid-Atlantic Ridge, but there are also samples from the East Pacific Rise, Juan de Fuca Ridge, Central Indian Ridge, and Southwest Indian Ridge. The Ba isotope compositions measured for all MORB glasses vary between $\delta^{138/134}Ba = +0.02$ and +0.15‰, which is at least twice the long-term repeatability of the technique (*22*). There are no systematic geographic differences in Ba isotope compositions and no correlation with Ba concentrations (table S1 and S2). Instead, we observe hyperbolic mixing relationships between Ba isotopes and $^{87}Sr/^{86}Sr$, $^{143}Nd/^{144}Nd$, and La/Sm, whereby the E-MORB end-member is characterized by $\delta^{138/134}Ba \sim +0.03 \pm 0.02$‰, and the D-MORB end-member is characterized by $\delta^{138/134}Ba \sim +0.14 \pm 0.02$‰ (Fig. 3).

We also report Ba isotope data for modern core-top sediments and AOC samples from two drill holes (table S4) to characterize the likely Ba isotope composition of subducted sediments and AOC. The core top sediments cover a broad range of geographical areas (Fig. 2), water depths, and Ba concentrations (table S4), which suggests that these samples represent much of the Ba isotope variations found in sediments. The relatively small Ba isotope variation found in these samples probably reflects that the Ba found in many similar types of marine sediments is dominated by the mineral barite that precipitates from seawater (*20*), which displays only moderate Ba isotope variation in most of the ocean (*22*).

The AOC samples represent shallow oceanic crust altered at low temperature [Deep Sea Drilling Project (DSDP) 442B samples (*38*)] and the deeper-sheeted dike complex [Ocean Drilling Program (ODP) 504B samples (*39*)] that is hydrothermally altered at high temperatures. Thus, the samples were selected to cover the different alteration styles likely encountered in subducted AOC. The large variation observed in the sample set strongly implies that some Ba isotope fractionation occurs during ocean crust alteration. The detailed mechanisms responsible for these isotope fractionations, however, are beyond the scope of the present study.

DISCUSSION

Origin of Ba isotope variation in MORB

The observed Ba isotope variation of MORBs could be caused by a number of different processes, including contamination by deep

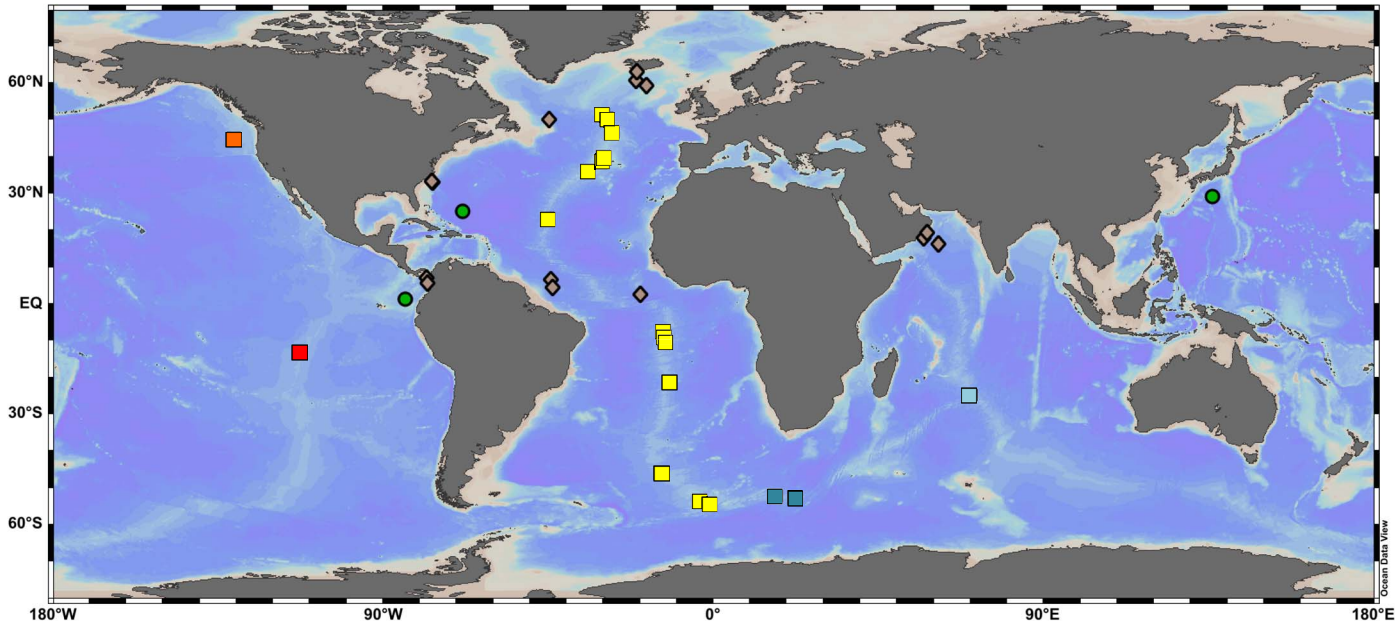

Fig. 2. Map of different samples investigated for Ba isotopes in this study. Squares are MORB glasses, green circles are AOC, and brown diamonds are sediments. MORB glasses are color-coded according to the ridge system/ocean basin they represent, and the same colors are used in Figs. 3 and 4.

mantle reservoirs, assimilation of shallow crustal materials during magma ascent, high-temperature stable isotope fractionation during melting and/or fractional crystallization, and last, crustal recycling processes. In the following, we argue that only the latter process is likely to explain our data set.

The Ba isotope variation of MORB observed here cannot reflect influence from deep mantle reservoirs with or without ancient recycled material. Anomalous He isotope compositions of mantle-derived melts (both higher and lower than MORB) are often interpreted to reflect influence from deep mantle reservoirs that may contain ancient recycled crustal materials. However, almost all samples investigated here record N-MORB He isotope ratios (table S1), suggesting that deep mantle reservoirs did not play a significant role in their source regions. In addition, the two samples with the lowest and highest $^{3}He/^{4}He$ (5.70 and 9.04 R_A, respectively; table S1) do not have anomalous Ba isotope compositions compared to the remainder of the samples, which further supports the absence of anomalous Ba isotope compositions from deep mantle reservoirs in the data set.

We also rule out assimilation as a likely cause for the observed Ba isotope variation. Because of the relatively high MgO concentrations for the studied samples (most samples exhibit MgO > 7.5%; table S3), assimilation of hydrothermal AOC is expected to be limited. Nonetheless, given that Ba is a highly incompatible element, it is possible that MORB melts with low initial Ba concentrations are particularly sensitive to assimilation. This process would be consistent with the observation that all the heaviest Ba isotope compositions are found for samples with Barium concentrations that are <25 μg/g. As a consequence, the assimilant (presumably AOC) should be characterized by heavy Ba isotope compositions, which is consistent with the data for AOC presented here (table S4) and elsewhere (*34*). However, AOC is also characterized by more radiogenic Sr isotope compositions relative to unaltered MORB, and thus, the highest $\delta^{138/134}Ba_{NIST}$ values should also be accompanied by more radiogenic $^{87}Sr/^{86}Sr$ (fig. S1) because Sr/Ba of AOC and MORB are similar (*30*, *31*). There is no association of heavy Ba isotopes with more radiogenic Sr isotopes, and heavy Ba isotope compositions are almost exclusively found in samples with unradiogenic $^{87}Sr/^{86}Sr \sim 0.7024$ (Fig. 3D), which is opposite from the trend expected from assimilation processes.

Stable isotope fractionation of Ba during melting of the DMM is also not a viable explanation for the isotopic variability of global MORBs, given that Ba is a highly incompatible trace element with a bulk partition coefficient during mantle melting of $D \sim 0.00012$ (*17*). Therefore, >99% of Ba will be in the melt after ~1% partial melting. Given that the entire range of MORBs represents degrees of melting between 6 and 20% (*40*, *41*), it follows that the net Ba isotope fractionation between the starting mantle composition and the resulting melt will be negligible. By the same reasoning, metasomatism and melt-rock reactions would similarly be incapable of producing the observed Ba isotope variations (see the Supplementary Materials).

Given the above arguments, the Ba isotope data presented here for MORBs can only be explained by addition of an isotopically distinct Ba component to the upper mantle that generated an EMM reservoir. The range of Ba isotope values observed for MORB represents mixtures between melts extracted from the enriched MORB mantle (EMM), characterized by $\delta^{138/134}Ba \approx 0.03‰$ and generally high Ba concentrations, and DMM, characterized by $\delta^{138/134}Ba \approx 0.14‰$ and generally low Ba concentrations. Mixing calculations between average D-MORB and E-MORB melt compositions show that the data are consistent with these mixing relationships (Fig. 3), supporting our contention that Ba isotope variation in MORBs derives from exchange between DMM and surface reservoirs.

Mixing between DMM and a light Ba source can reconcile the overall patterns between several trace elements (for example, Rb/Sr and La/Sm), radiogenic (for example, Sr and Nd), and Ba stable isotope data, albeit with some scatter outside the narrowly defined mixing lines that are calculated, assuming complete homogeneity of the EMM and DMM reservoirs. In detail, this assumption is not justified as melt depletion, and mantle enrichment processes would without doubt generate some heterogeneity in both trace element concentrations and radiogenic isotope ratios. Hence, it is not surprising to find some outliers

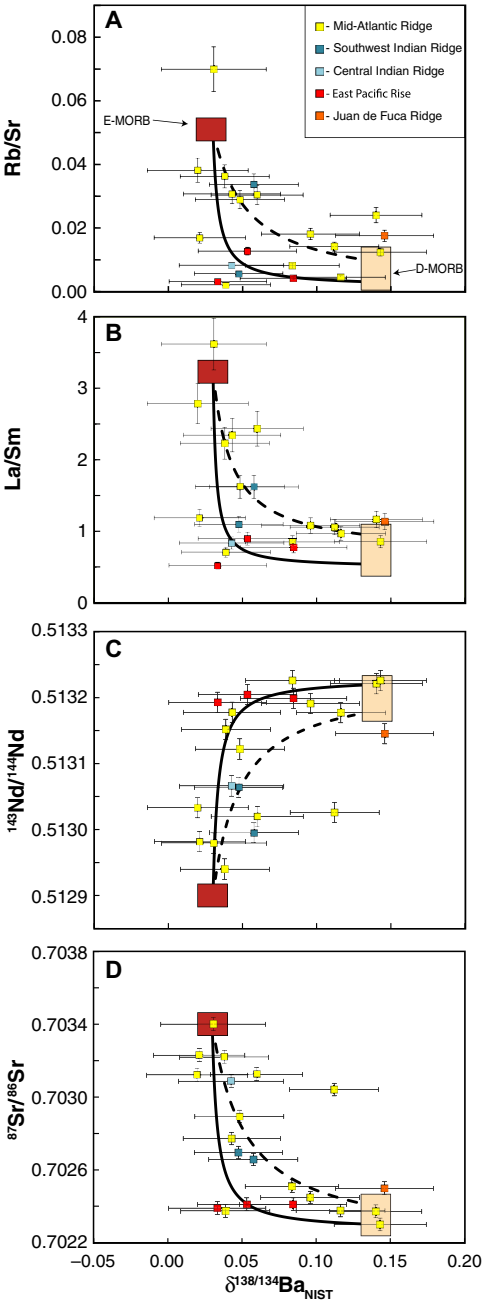

Fig. 3. Barium isotope data for MORB and melt mixing at the ridge. Barium isotope data for MORB glasses plotted against (**A**) Rb/Sr ratios, (**B**) La/Sm ratios, (**C**) Nd isotopes, and (**D**) Sr isotopes. Also shown are mixing lines between two different D-MORB compositions [see (*3*) and most depleted sample from this study] and E-MORB (*3*) melts (bold and dashed black lines). These mixing lines show that all the isotopic and trace element data can be explained via mixing between two distinct end-member melts at the mid-ocean ridge. Error bars for isotope ratios are 2 SDs, and trace element ratios are ±10%.

from the idealized mixing lines presented in Figs. 3 and 4. The scatter outside the E-MORB to D-MORB mixing lines is particularly strong for trace element ratios that show relatively little overall variation in global MORB such as Ba/Th and Ce/Pb (Fig. 4), but this is expected given the small differences between EMM and DMM for these trace element ratios. However, considering that different regions of DMM and EMM were generated by a distinct set of processes (for example, melt depletion and mantle refertilization events), it is remarkable that MORB samples from all regions around the globe broadly fit a single mixing relationship between Ba isotopes and other indicators of mantle enrichment. This observation strongly implies that the material with relatively uniform Ba isotope compositions was responsible for producing the EMM reservoirs.

To identify the source of isotopically light Ba contaminating the mantle, we surveyed modern sediments and AOC for their Ba isotope compositions. We examined 31 modern core top sediments from different locations around the globe, with a total of 11: altered basalts from ODP Hole 504B and DSDP Hole 442B, as well as the supercomposite (*42*) from DSDP Hole 417/418 (table S4). We find that the average sediment Ba isotope composition is $\delta^{138/134}$Ba = 0.01‰ (±0.04 SD, n = 31; table S4), within error of the E-MORB value of $\delta^{138/134}$Ba ≈ 0.03‰. This value is identical to that recently found for an extensive survey of South Atlantic bulk sediments (*28*). The altered basalt samples display a large range of values from $\delta^{138/134}$Ba = −0.09 to +0.33‰. Because of the narrow range and strong similarity between sedimentary and E-MORB Ba isotopes, it is reasonable to conclude that the Ba isotope variations observed in global MORB are most likely due to addition of sediment material to the upper mantle. In contrast, the large Ba isotope variation observed for AOC relative to EMM (Fig. 1) implies that AOC did not contribute significantly to the Ba budget of EMM. This conclusion is also supported by quantitative mixing calculations between DMM and AOC (fig. S1) that predict a much wider range in Ba isotopes for MORB than observed. However, even if average AOC uniformly yielded a value of $\delta^{138/134}$Ba ~ 0.05, similar to the DSDP 417/418 supercomposite (table S4), then unradiogenic ^{87}Sr/^{86}Sr and light Ba isotope compositions would not be produced with DMM-AOC mixing (fig. S1) because of the radiogenic ^{87}Sr/^{86}Sr found in AOC due to hydrothermal alteration (*30*, *31*). Thus, AOC addition would not be able to simultaneously account for all the Sr and Ba isotope compositions. In addition, Nd isotopes would likely be unaffected by AOC mixing because hydrothermal alteration does not modify Nd isotopes. Hence, sufficient AOC mixing could produce Sr and Ba isotope values broadly similar to the EMM end-member, whereas Nd isotopes could not be. The Sr-Ba mixing lines (fig. S1) would remain almost identical if, instead of bulk AOC addition, hydrous AOC melts were considered because Ba/Sr is not significantly fractionated during partial melting of AOC at high pressures and temperatures (*18*). It should be noted that the lack of influence on Ba isotopes from AOC does not preclude the presence of recycled oceanic crust in the source of MORB (*7*). However, since sediments contain one to two orders of magnitude more Ba than oceanic crust (*20*), our Ba isotope composition for MORB is overwhelmingly controlled by sediment addition rather than AOC.

Mechanisms of sediment addition to the upper mantle

The fact that addition of sediment-rich material appears to be global in nature indicates that subduction zones are the most likely setting where transfer of sedimentary Ba occurs. By combining Ba isotope signatures with radiogenic isotopes and trace element systematics of the MORBs (see the Supplementary Materials for details), we can further constrain the sequence of events leading to EMM formation.

To do this, we calculate the concentrations of the trace elements Ba, Rb, Sr, La, Ce, Nd, Sm, Pb, and Th for different sediment components that might be released from a subducted slab into the mantle wedge (Fig. 4). We construct mixing relationships for terrigenous sediments, pelagic clays, and global subducted sediment (GLOSS) (*20*). Fluid compositions were only calculated for Ba and Th, as these two elements

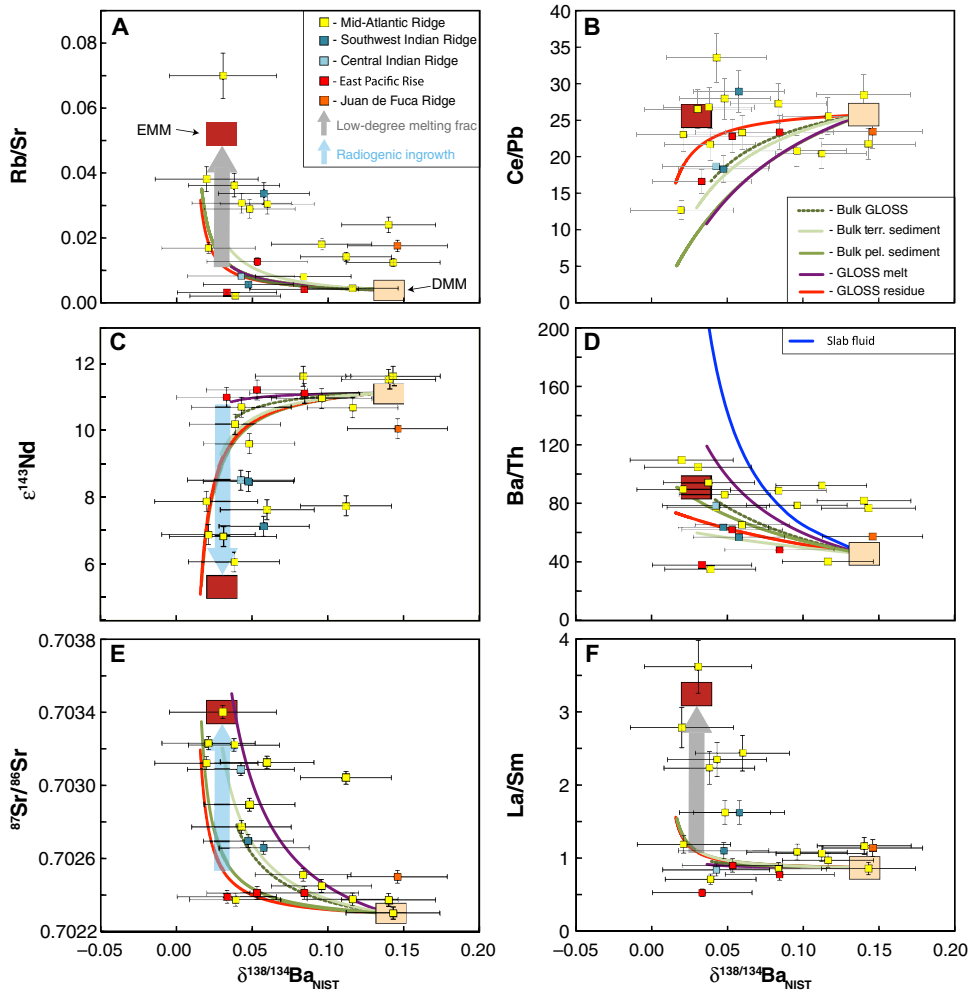

Fig. 4. Barium isotope data for MORB and sediment addition in a subduction zone. Barium isotope data for MORB glasses plotted against (**A**) Rb/Sr ratios, (**B**) Ce/Pb ratios, (**C**) Nd isotopes, (**D**) Ba/Th ratios, (**E**) Sr isotopes, and (**F**) La/Sm ratios. Also shown are mixing lines between the DMM (*17*, *52*) and sediment-rich components derived from subducting slabs. These mixing lines indicate the processes taking place in subduction zones that could be capable of producing the EMM reservoir. The mixing lines for bulk pelagic (pel.) clay, bulk terrigenous (terr.) sediment, bulk global subducted sediment (GLOSS), GLOSS melt, and residues of GLOSS melting are stopped at 0.4, 0.3, 0.1, 0.08, and 0.8% addition to the DMM, respectively. Sediment compositions are average subducted pelagic/brown clays, terrigenous/turbidite sediments, and GLOSS (*20*). Partition coefficients for Ba and Th in slab fluids released at 4 GPa and 800°C (*18*) are assumed to represent 10% fluid release from GLOSS. Partition coefficients for Ba, Th, La, Nd, and Sm during GLOSS melting assume 10% batch melting at 3.5 GPa and 900°C (*43*). Residual sediment calculations assume that 50% of the sediment is removed at 3.5 GPa and 900°C before mixing with the DMM. The degrees of melting and fluid release used to construct the mixing lines are not critical as different melt and fluid fractions produce broadly similar results.

display highly disparate affinities for aqueous subduction zone fluids (*18*). Sediment melts were calculated from 10% batch melting of GLOSS using the average partition coefficients of two experiments at 900°C and 3.5 GPa, where a complete data set of all elements considered here was presented (*43*). Other studies have found similar partition coefficients for sediment melting (*44*, *45*), with the notable exception of Pb, which likely produced somewhat erroneous results due to loss to the capsule during the experiments (*43*). Given that Pb is expected to behave similarly to Sr (*43*), which has a melt-solid K_d ~ 7.5, we here infer a melt-solid K_d ~ 5 for Pb during sediment melting (table S5). Residues of sediment melting used the same partition coefficients as the sediment melting calculations, but it was assumed that 50% of the mass of the original sediment had been removed during arc magma generation before adding sediment residue to the depleted mantle.

There is currently significant debate regarding the nature of the subducted slab at depth in subduction zones. Field evidence, modeling, and geochemical data point toward mélange material playing a key role in arc lava genesis (*46*–*48*), which suggests that pure sediment melting as modeled here possibly does not take place in subduction zones. Recent experiments of mélange melting (*49*) have shown that trace element fractionation similar to that of pure sediment melting is possible under a range of conditions. However, further work is needed before quantitative models of mélange melting can be applied to the formation mechanisms of the E-MORB reservoir.

Our modeling shows, in agreement with previous studies (*5*), that the mechanism of sediment Ba addition to the upper mantle was not via fluids because high Ba/Th ratios in the E-MORB samples are not observed (Fig. 4D, blue line), which would be expected since aqueous

subduction zone fluids should be characterized by extremely high Ba/Th (*18*). Furthermore, addition of 0.08% by weight of partial sediment melts to the DMM would change the Ba isotope composition to the EMM value (Fig. 4, purple lines). However, this process would lead to more radiogenic Sr isotopes than EMM, whereas it would have no significant impact on the Nd isotope and La/Sm ratios (Fig. 4). Likewise, addition of 0.1 to 0.3% by weight of bulk terrigenous and GLOSS (*20*) would produce Ba and Sr isotope values similar to EMM but would again not significantly change trace element ratios or Nd isotopes (Fig. 4, green lines). Mixing 0.4% bulk pelagic clay (*20*) or 0.8% slab residues left after extraction of arc magmas with DMM produces Ba, Sr, and Nd isotope compositions largely similar to EMM. However, at these degrees of mixing, several trace element ratios (for example, Ce/Pb, La/Sm, and Rb/Sr) would be much lower than the ranges found in MORB. Thus, there are no direct mixing processes between a sediment-rich component and DMM that could reproduce the observed relationships between Ba, Sr, and Nd isotopes and trace element ratios (Fig. 4). In particular, neither Rb/Sr ratios (Fig. 4) nor Sm/Nd ratios (not shown) would change sufficiently for Nd and Sr isotope ratios of the DMM to evolve with time to the values observed in E-MORB. As suggested by a previous work (*5*), trace element ratios involving Pb (for example, Ce/Pb) are affected to some degree by sediment mixing processes. However, the amounts of sediment needed to shift Ba isotopes will not change these trace element ratios beyond the range of values observed for D-MORB and E-MORB in general (Fig. 4).

To explain the Ba, Sr, and Nd isotopic and trace element systematics of MORBs, a process is required where trace element ratios are strongly fractionated at the same time that sedimentary Ba is added into the mantle. We argue that the introduction of sediment-rich material, likely in the form of melts from subducted slab residues (Fig. 5), induces low-degree (<1%) melting of DMM in subduction zones. Most likely, the incipient melting would be initiated because the sedimentary component contains more water than the depleted mantle. However, the small volume of the enriched low-degree melts would prohibit them from percolating large distances in the upper mantle, and they would freeze back into the mantle above the slab. This process would generate a new enriched reservoir, equivalent to an EMM, characterized by highly fractionated La/Sm, Rb/Sr, and Sm/Nd, as well as the Ba isotope composition of sediments. Subsequently, these domains of fractionated trace elements and light Ba isotopes would require ~100 to 500 million years (Ma) to evolve to Sr and Nd isotope compositions similar to those found in E-MORB (*5*).

Pervasive presence of sediment Ba in the upper mantle

The chemical budget of the upper mantle that can be traced to sediment-derived material differs for each element because the relative concentrations of mantle and sediment vary by many orders of magnitude. Since the budget of Ba is so strongly controlled by sedimentary inputs, however, it is a unique tool to trace recycling. The most comprehensive study of global MORBs (*3*) has shown that the average composition of MORBs is

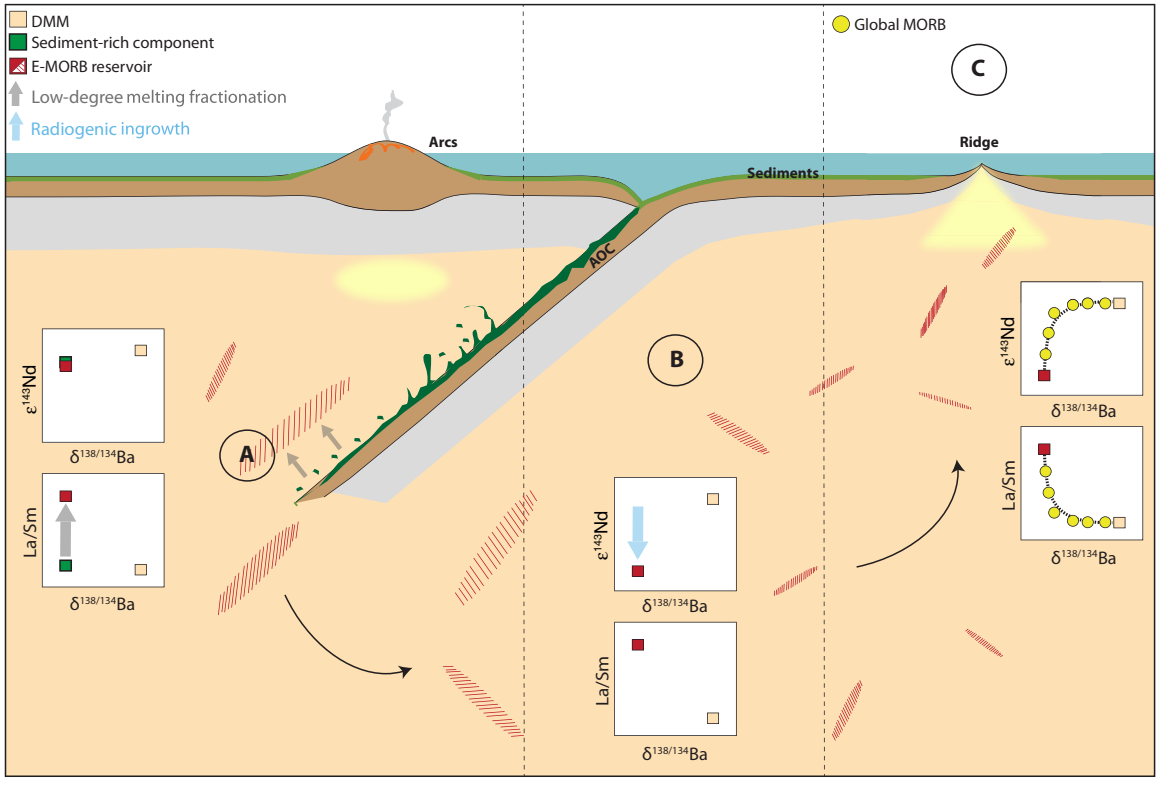

Fig. 5. Simplified geodynamic schematic of EMM generation. (**A**) During subduction, a hydrous sediment-rich component is added at depth to the DMM. Addition of this component triggers incipient partial melting of the DMM (arrow from green to red square). These low-degree partial melts that are contaminated by sedimentary Ba freeze back into the mantle and create the EMM reservoir. (**B**) Convection of the upper mantle for 100 to 500 Ma causes radiogenic ingrowth (downward arrow) in the EMM reservoir that diverges from the DMM. (**C**) Melting at ridges generates melts from EMM and DMM that mix in variable proportions to produce hyperbolic mixing relationships between Ba, Nd isotopes, and La/Sm element ratios.

enriched compared to D-MORB, with $^{87}Sr/^{86}Sr$ ~ 0.70282 and $^{143}Nd/^{144}Nd$ ~ 0.51307. Given the correlations between Ba, Nd, and Sr isotopes (Fig. 3), we can infer that the average Ba isotope composition of global MORB is likely $\delta^{138/134}Ba$ ~ 0.04 to 0.06‰, which, given D-MORB and sedimentary Ba isotope compositions of $\delta^{138/134}Ba$ ~ 0.14 and 0.01, respectively, implies that ~60 to 80% of all Ba in the upper mantle originates from sediments. On the other hand, the fraction of the pure E-MORB component in average MORB would only be 3 to 20% because of the much higher Ba concentrations in E-MORB. In the upper mantle, the proportion of elements that originate from sedimentary material will vary for different elements, but because Ba is so strongly controlled by sedimentary material, that makes it a unique tool to trace pervasive sediment recycling. Thus, using Ba isotope signatures of MORBs away from plume influence, we demonstrate that subducted sediments play a key role in the formation of E-MORB reservoir and that most melts from the upper mantle contain minor amounts (<0.1%) of recycled sediment.

MATERIALS AND METHODS

All samples were prepared for elemental and isotopic analyses at the Non-traditional Isotope Research for Advanced Novel Applications (NIRVANA) Laboratories at the Woods Hole Oceanographic Institution (WHOI). Barium was separated from the sample matrix using cation exchange chromatographic resin (AGWX50, 200 to 400 mesh) in 2 M HCl (*22*). Barium isotope compositions of MORB glasses, AOC, and sediment core tops were measured using a ThermoFinnigan Neptune MC-ICP-MS (multicollector inductively coupled plasma mass spectrometer) situated in the WHOI Plasma Facility. Instrumental and sample mass fractionation was monitored and corrected using a ^{135}Ba-^{136}Ba double spike, which achieves a long-term 2 SD precision for sample unknowns of ±0.03‰ (*24*, *50*). The ^{135}Ba-^{136}Ba double spike has a $^{136}Ba/^{135}Ba$ ratio of 0.997917 ± 0.000099 (±2 SD); ^{138}Ba and ^{137}Ba are minor constituents of the spike, contributing ≈3.9 and 1.3 % of the total Ba. Barium isotope compositions were reported relative to the NIST Standard Reference Materials 3104a standard using conventional delta notation. Additional details regarding the mass spectrometric technique and assessment of long-term analytical precision and accuracy are provided in the Supplementary Materials. Isotope compositions of Sr and Nd were similarly determined for a subset of the samples (table S1) via MC-ICP-MS using previously described methods that yield uncertainties of ±30 parts per million (ppm) for $^{143}Nd/^{144}Nd$ and ±50 ppm for $^{87}Sr/^{86}Sr$ (*51*).

Trace element concentrations were determined for all samples using a ThermoFinnigan ELEMENT 2 sector-field ICP-MS, also situated at the WHOI Plasma Facility. Concentrations were calculated via reference to ion beam intensities obtained from a five-point calibration curve constructed from serial dilutions of a gravimetrically prepared multielement standard; drift was monitored and corrected via normalization to indium intensities. Accuracy and precision were determined to be better than ±5% (SD) based on the correspondence between highly precise Ba concentrations determined via the double spiking technique and the ICP-MS. We also measured several of the major and minor elements by ICP-MS (Mg, Ca, Fe, Ti, Mn, and P) and report these for the samples where major elements had not previously been measured (table S3). There is good agreement between major and minor elements measured by ICP-MS (this study) and electron microprobe (EMP), although the concentrations measured by ICP-MS tend to be higher by, on average, 7% compared with the literature EMP measurements. These small differences and the scatter in the correlation between electron probe and ICP-MS could be due to sample heterogeneity, the larger uncertainties on the ICP-MS measurements, or small inaccuracies in either measurement technique. However, for the purposes of our study, the difference between the two data sets was inconsequential.

SUPPLEMENTARY MATERIALS

Supplementary material for this article is available at http://advances.sciencemag.org/cgi/content/full/4/7/eaas8675/DC1

Table S1. Isotope data for MORB glass samples.
Table S2. Trace element data for MORB glasses in microgram per gram.
Table S3. Major element compositions of MORB glasses.
Table S4. Barium isotope data for AOC and sediment core tops.
Table S5. Partition coefficients used to calculate sediment melting.
Table S6. Barium isotope data for international reference materials.
Fig. S1. Barium isotopes plotted against Sr isotopes for MORB samples.
Fig. S2. Calculated Ba isotope variation in MORB mantle reservoirs generated by hypothetical isotope fractionation during melt depletion.
References (*53*–*71*)

REFERENCES AND NOTES

1. A. W. Hofmann, W. M. White, Mantle plumes from ancient oceanic crust. *Earth Planet. Sci. Lett.* **57**, 421–436 (1982).
2. A. W. Hofmann, in *Treatise on Geochemistry (Second Edition)*, D. Holland, K. K. Turekian Heinrich, Eds. (Elsevier, 2014), pp. 67–101.
3. A. Gale, C. A. Dalton, C. H. Langmuir, Y. Su, J.-G. Schilling, The mean composition of ocean ridge basalts. *Geochem. Geophys. Geosyst.* **14**, 489–518 (2013).
4. P. J. Michael, R. L. Chase, The influence of primary magma composition, H_2O and pressure on midocean ridge basalt differentiation. *Contrib. Mineral. Petrol.* **96**, 245–263 (1987).
5. K. E. Donnelly, S. L. Goldstein, C. H. Langmuir, M. Spiegelman, Origin of enriched ocean ridge basalts and implications for mantle dynamics. *Earth Planet. Sci. Lett.* **226**, 347–366 (2004).
6. P. D. Asimow C. H. Langmuir, The importance of water to oceanic mantle melting regimes. *Nature* **421**, 815–820 (2003).
7. J. M. Eiler, P. Schiano, N. Kitchen, E. M. Stolper, Oxygen-isotype evidence for recycled crust in the sources of mid-ocean-ridge basalts. *Nature* **403**, 530–534 (2000).
8. Y. Niu, K. D. Collerson, R. Batiza, J. I. Wendt, M. Regelous, Origin of enriched-type mid-ocean ridge basalt at ridges far from mantle plumes: The East Pacific Rise at 11° 20′N. *J. Geophys. Res.* **104**, 7067–7087 (1999).
9. M. D. Kurz, A. P. Le Roex, H. J. B. Dick, Isotope geochemistry of the oceanic mantle near the Bouvet triple junction. *Geochim. Cosmochim. Acta* **62**, 841–852 (1998).
10. M. D. Kurz, W. J. Jenkins, J. G. Schilling, S. R. Hart, Helium isotopic variations in the mantle beneath the Central-North Atlantic-Ocean. *Earth Planet. Sci. Lett.* **58**, 1–14 (1982).
11. D. W. Graham, W. J. Jenkins, J.-G. Schilling, G. Thompson, M. D. Kurz, S. E. Humphris, Helium isotope geochemistry of midocean ridge basalts from the South-Atlantic. *Earth Planet. Sci. Lett.* **110**, 133–147 (1992).
12. C. L. Waters, K. W. W. Sims, M. R. Perfit, J. Blichert-Toft, J. Blusztajn, Perspective on the genesis of E-MORB from chemical and isotopic heterogeneity at 9–10°N East Pacific Rise. *J. Petrol.* **52**, 565–602 (2011).
13. D. Mckenzie, R. K. Onions, Mantle reservoirs and ocean island basalts. *Nature* **301**, 229–231 (1983).
14. M. M. Hirschmann, E. M. Stolper, A possible role for garnet pyroxenite in the origin of the "garnet signature" in MORB. *Contrib. Mineral. Petrol.* **124**, 185–208 (1996).
15. J. P. Morgan, W. J. Morgan, Two-stage melting and the geochemical evolution of the mantle: A recipe for mantle plum-pudding. *Earth Planet. Sci. Lett.* **170**, 215–239 (1999).
16. M. Rehkämper, A. W. Hofmann, Recycled ocean crust and sediment in Indian Ocean MORB. *Earth Planet. Sci. Lett.* **147**, 93–106 (1997).
17. R. K. Workman, S. R. Hart, Major and trace element composition of the depleted MORB mantle (DMM). *Earth Planet. Sci. Lett.* **231**, 53–72 (2005).
18. R. Kessel, M. W. Schmidt, P. Ulmer, T. Pettke, Trace element signature of subduction-zone fluids, melts and supercritical liquids at 120–180 km depth. *Nature* **437**, 724–727 (2005).
19. T. Elliott, in *Geophysical Monograph*, J. Eiler, Ed. (American Geophysical Union, 2003), vol. 138, pp. 23–45.
20. T. Plank, C. H. Langmuir, The chemical composition of subducting sediment and its consequences for the crust and mantle. *Chem. Geol.* **145**, 325–394 (1998).
21. K. von Allmen, M. E. Böttcher, E. Samankassou, T. F. Nagler, Barium isotope fractionation in the global barium cycle: First evidence from barium minerals and precipitation experiments. *Chem. Geol.* **277**, 70–77 (2010).
22. T. J. Horner, C. W. Kinsley, S. G. Nielsen, Barium-isotopic fractionation in seawater mediated by barite cycling and oceanic circulation. *Earth Planet. Sci. Lett.* **430**, 511–522 (2015).

23. Y.-T. Hsieh, G. M. Henderson, Barium stable isotopes in the global ocean: Tracer of Ba inputs and utilization. *Earth Planet. Sci. Lett.* **473**, 269–278 (2017).
24. S. L. Bates, K. R. Hendry, H. V. Pryer, C. W. Kinsley, K. M. Pyle, E. M. S. Woodward, T. J. Horner, Barium isotopes reveal role of ocean circulation on barium cycling in the Atlantic. *Geochim. Cosmochim. Acta* **204**, 286–299 (2017).
25. T. Bullen, O. Chadwick, Ca, Sr and Ba stable isotopes reveal the fate of soil nutrients along a tropical climosequence in Hawaii. *Chem. Geol.* **422**, 25–45 (2016).
26. K. van Zuilen, T. Müller, T. F. Nägler, M. Dietzel, T. Küsters, Experimental determination of barium isotope fractionation during diffusion and adsorption processes at low temperatures. *Geochim. Cosmochim. Acta* **186**, 226–241 (2016).
27. A. E. Hofmann, I. C. Bourg, D. J. DePaolo, Ion desolvation as a mechanism for kinetic isotope fractionation in aqueous systems. *Proc. Natl. Acad. Sci. U.S.A.* **109**, 18689–18694 (2012).
28. L. Bridgestock, Y.-T. Hsieh, D. Porcelli, W. B. Homoky, A. Bryan, G. M. Henderson, Controls on the barium isotope compositions of marine sediments. *Earth Planet. Sci. Lett.* **481**, 101–110 (2018).
29. L. H. Chan, D. Drummond, J. M. Edmond, B. Grant, On the barium data from the Atlantic GEOSECS expedition. *Deep Sea Res.* **24**, 613–649 (1977).
30. H. Staudigel, S. R. Hart, Alteration of basaltic glass: Mechanisms and significance for the oceanic-crust seawater budget. *Geochim. Cosmochim. Acta* **47**, 337–350 (1983).
31. K. A. Kelley, T. Plank, J. Ludden, H. Staudigel, Composition of altered oceanic crust at ODP sites 801 and 1149. *Geochem. Geophys. Geosyst.* **4**, 1–21 (2003).
32. D. A. H. Teagle, J. C. Alt, A. N. Halliday, Tracing the chemical evolution of fluids during hydrothermal recharge: Constraints from anhydrite recovered in ODP Hole 504B. *Earth Planet. Sci. Lett.* **155**, 167–182 (1998).
33. R. D. Shannon, Revised effective ionic radii and systematic studies of interatomic distances in halides and chalcogenides. *Acta Crystallogr.* **A32**, 751–767 (1976).
34. X. Y. Nan, H. M. Yu, Y. J. Gao, Barium isotope composition of altered oceanic crust from the IODP Site 1256 at the East Pacific Rise, paper presented at the AGU Fall Meeting, New Orleans, LA, 13 December 2017.
35. M. D. Kurz, W. J. Jenkins, The distribution of helium in oceanic basalt glasses. *Earth Planet. Sci. Lett.* **53**, 41–54 (1981).
36. J. E. Georgen, M. D. Kurz, H. J. B. Dick, J. Lin, Low $^{3}He/^{4}He$ ratios in basalt glasses from the western Southwest Indian Ridge (10°-24°E). *Earth Planet. Sci. Lett.* **206**, 509–528 (2003).
37. C. M. Meyzen, J. Blichert-Toft, J. N. Ludden, E. Humler, C. Mével, F. Albarède, Isotopic portrayal of the Earth's upper mantle flow field. *Nature* **447**, 1069–1074 (2007).
38. Y. Shu, S. G. Nielsen, Z. Zeng, R. Shinjo, J. Blusztajn, X. Wang, S. Chen, Tracing subducted sediment inputs to the Ryukyu arc-Okinawa trough system: Evidence from thallium isotopes. *Geochim. Cosmochim. Acta* **217**, 462–491 (2017).
39. W. Bach, B. Peucker-Ehrenbrink, S. R. Hart, J. S. Blusztajn, Geochemistry of hydrothermally altered oceanic crust: DSDP/ODP Hole 504B—Implications for seawater-crust exchange budgets and Sr- and Pb-isotopic evolution of the mantle. *Geochem. Geophys. Geosyst.* **4**, 1–29 (2003).
40. E. M. Klein, C. H. Langmuir, Global correlations of ocean ridge basalt chemistry with axial depth and crustal thickness. *J. Geophys. Res.* **92**, 8089–8115 (1987).
41. A. W. Hofmann, Chemical differentiation of the Earth: The relationship between mantle, continental crust, and oceanic crust. *Earth Planet. Sci. Lett.* **90**, 297–314 (1988).
42. H. Staudigel, G. R. Davies, S. R. Hart, K. M. Marchant, B. M. Smith, Large scale isotopic Sr, Nd and O isotopic anatomy of altered oceanic crust: DSDP/ODP sites 417/418. *Earth Planet. Sci. Lett.* **130**, 169–185 (1995).
43. J. Hermann, D. Rubatto, Accessory phase control on the trace element signature of sediment melts in subduction zones. *Chem. Geol.* **265**, 512–526 (2009).
44. S. Skora, J. Blundy, High-pressure hydrous phase relations of radiolarian clay and implications for the involvement of subducted sediment in arc magmatism. *J. Petrol.* **51**, 2211–2243 (2010).
45. M. C. Johnson, T. Plank, Dehydration and melting experiments constrain the fate of subducted sediments. *Geochem. Geophys. Geosyst.* **1**, 1–26 (1999).
46. G. E. Bebout, Metamorphic chemical geodynamics of subduction zones. *Earth Planet. Sci. Lett.* **260**, 373–393 (2007).
47. H. R. Marschall, J. C. Schumacher, Arc magmas sourced from mélange diapirs in subduction zones. *Nat. Geosci.* **5**, 862–867 (2012).
48. S. G. Nielsen, H. R. Marschall, Geochemical evidence for mélange melting in global arcs. *Sci. Adv.* **3**, e1602402 (2017).
49. A. M. Cruz-Uribe, H. R. Marschall, G. A. Gaetani, V. Le Roux, Generation of alkaline magmas in subduction zones by melting of mélange diapirs—An experimental study. *Geology* **46**, 343–346 (2018).
50. T. J. Horner, H. V. Pryer, S. G. Nielsen, P. W. Crockford, J. M. Gauglitz, B. A. Wing, R. D. Ricketts, Pelagic barite precipitation at micromolar ambient sulfate. *Nat Commun.* **8**, 1342 (2017).
51. S. G. Nielsen, G. Yogodzinski, J. Prytulak, T. Plank, S. M. Kay, R. W. Kay, J. Blusztajn, J. D. Owens, M. Auro, T. Kading, Tracking along-arc sediment inputs to the Aleutian arc using thallium isotopes. *Geochim. Cosmochim. Acta* **181**, 217–237 (2016).
52. V. J. M. Salters, A. Stracke, Composition of the depleted mantle. *Geochem. Geophys. Geosyst.* **5**, Q05004 (2004).
53. Z. Cao, C. Siebert, E. C. Hathorne, M. Dai, M. Frank, Constraining the oceanic barium cycle with stable barium isotopes. *Earth Planet. Sci. Lett.* **434**, 1–9 (2016).
54. N. Saito, Selected data on ion exchange separations in radionalytical chemistry. *Pure Appl. Chem.* **56**, 523–539 (1984).
55. W. F. McDonough, S.-s. Sun, The composition of the Earth. *Chem. Geol.* **120**, 223–253 (1995).
56. K. T. M. Johnson, H. J. B. Dick, N. Shimizu, Melting in the oceanic upper mantle: An ion microprobe study of diopsides in abyssal peridotites. *J. Geophys. Res.* **95**, 2661–2678 (1990).
57. A. P. Leroex, H. J. B. Dick, A. J. Erlank, A. M. Reid, F. A. Frey, S. R. Hart, Geochemistry, mineralogy and petrogenesis of lavas erupted along the southwest Indian Ridge between the Bouvet Triple Junction and 11-degrees east. *J. Petrol.* **24**, 267–318 (1983).
58. D. Fontignie, J.-G. Schilling, Mantle heterogeneities beneath the South Atlantic: A Nd-Sr-Pb isotope study along the Mid-Atlantic Ridge (3°S–46°S). *Earth Planet. Sci. Lett.* **142**, 209–221 (1996).
59. K. A. Kelley, R. Kingsley, J.-G. Schilling, Composition of plume-influenced mid-ocean ridge lavas and glasses from the Mid-Atlantic Ridge, East Pacific Rise, Galapagos Spreading Center, and Gulf of Aden. *Geochem. Geophys. Geosyst.* **14**, 223–242 (2013).
60. M. D. Kurz, M. Moreira, J. Curtice, D. E. Lott III, J. J. Mahoney, J. M. Sinton, Correlated helium, neon, and melt production on the super-fast spreading East Pacific Rise near 17° S. *Earth Planet. Sci. Lett.* **232**, 125–142 (2005).
61. J. J. Mahoney, J. M. Sinton, M. D. Kurz, J. D. Macdougall, K. J. Spencer, G. W. Lugmair, Isotope and trace-element characteristics of a super-fast spreading ridge: East Pacific Rise, 13–23°S. *Earth Planet. Sci. Lett.* **121**, 173–193 (1994).
62. W. M. White, W. B. Bryan, Sr-isotope, K, Rb, Cs, Sr, Ba, and rare-earth geochemistry of basalts from FAMOUS area. *Geol. Soc. Am. Bull.* **88**, 571–576 (1977).
63. J. Blichert-Toft, A. Agranier, M. Andres, R. Kingsley, J.-G. Schilling, F. Albarède, Geochemical segmentation of the Mid-Atlantic Ridge north of Iceland and ridge-hot spot interaction in the North Atlantic. *Geochem. Geophys. Geosyst.* **6**, Q01E19 (2005).
64. D. Yu, D. Fontignie, J.-G. Schilling, Mantle plume-ridge interactions in the Central North Atlantic: A Nd isotope study of Mid-Atlantic Ridge basalts from 30°N to 50°N. *Earth Planet. Sci. Lett.* **146**, 259–272 (1997).
65. W. G. Melson, T. O'Hearn, E. Jarosewich, A data brief on the Smithsonian Abyssal Volcanic Glass Data File. *Geochem. Geophys. Geosyst.* **3**, 1023 (2002).
66. A. Bézos, E. Humler, The $Fe^{3+}/\Sigma Fe$ ratios of MORB glasses and their implications for mantle melting. *Geochim. Cosmochim. Acta.* **69**, 711–725 (2005).
67. J. J. Standish, H. J. B. Dick, P. J. Michael, W. G. Melson, T. O'Hearn, MORB generation beneath the ultraslow spreading Southwest Indian Ridge (9–25°E): Major element chemistry and the importance of process versus source. *Geochem. Geophys. Geosyst.* **9**, Q05004 (2008).
68. J. M. Sinton, S. M. Smaglik, J. J. Mahoney, K. C. Macdonald, Magmatic processes at superfast spreading mid-ocean ridges: Glass compositional variations along the east pacific rise 13°-23°S. *J. Geophys. Res.* **96**, 6133–6155 (1991).
69. J. G. Schilling, M. Zajac, R. Evans, T. Johnston, W. White, J. D. Devine, R. Kingsley, Petrologic and geochemical variations along the mid-atlantic ridge from 29°N to 73°N. *Am. J. Sci.* **283**, 510–586 (1983).
70. K. van Zuilen, T. F. Nägler, T. D. Bullen, Barium isotopic compositions of geological reference materials. *Geostand. Geoanal. Res.* **40**, 543–558 (2016).
71. X. Nan, F. Wu, Z. Zhang, Z. Hou, F. Huang, H. Yu, High-precision barium isotope measurements by MC-ICP-MS. *J. Anal. At. Spectrom* **30**, 2307–2315 (2015).

Acknowledgments: We thank W. Bach for providing samples from ODP Hole 504B and E. Soucy for helping with sample digestions. This study used samples from the ocean drilling program. We thank M. Auro and the rest of the NIRVANA group at WHOI for keeping clean laboratories and the WHOI Plasma Mass Spectrometry Facility functioning at all times. **Funding:** This study was supported by NSF grants EAR-1119373 and EAR-1427310 to S.G.N. **Author contributions:** S.G.N. designed the study and selected samples together with M.D.K. Sample analysis was performed by T.J.H., H.V.P., Y.S., and J.B. S.G.N. and V.L.R. designed the figures and performed data interpretation with input from all co-authors. S.G.N. wrote the paper with input from V.L.R., T.J.H., and M.D.K. **Competing interests:** The authors declare that they have no competing interests. **Data and materials availability:** All data needed to evaluate the conclusions in the paper are present in the paper and/or the Supplementary Materials. Additional data related to this paper may be requested from the authors.

Submitted 27 December 2017
Accepted 31 May 2018
Published 11 July 2018
10.1126/sciadv.aas8675

Citation: S. G. Nielsen, T. J. Horner, H. V. Pryer, J. Blusztajn, Y. Shu, M. D. Kurz, V. Le Roux, Barium isotope evidence for pervasive sediment recycling in the upper mantle. *Sci. Adv.* **4**, eaas8675 (2018).

Science Advances

Barium isotope evidence for pervasive sediment recycling in the upper mantle

Sune G. Nielsen, Tristan J. Horner, Helena V. Pryer, Jerzy Blusztajn, Yunchao Shu, Mark D. Kurz and Véronique Le Roux

Sci Adv **4** (7), eaas8675.
DOI: 10.1126/sciadv.aas8675